



Influence of the annealing temperature on the photoluminescence of Er-doped SiO thin films

G. Wora Adeola, H. Rinnert, P. Miska, M. Vergnat

► To cite this version:

G. Wora Adeola, H. Rinnert, P. Miska, M. Vergnat. Influence of the annealing temperature on the photoluminescence of Er-doped SiO thin films. *Journal of Applied Physics*, 2007, 102 (5), pp.053515. <10.1063/1.2777203>. <hal-02164238>

HAL Id: hal-02164238

<https://hal.science/hal-02164238v1>

Submitted on 24 Jun 2019

HAL is a multi-disciplinary open access archive for the deposit and dissemination of scientific research documents, whether they are published or not. The documents may come from teaching and research institutions in France or abroad, or from public or private research centers.

L'archive ouverte pluridisciplinaire **HAL**, est destinée au dépôt et à la diffusion de documents scientifiques de niveau recherche, publiés ou non, émanant des établissements d'enseignement et de recherche français ou étrangers, des laboratoires publics ou privés.



HAL Authorization

Influence of the annealing temperature on the photoluminescence of Er-doped SiO thin films

G. Wora Adeola, H. Rinnert,^{a)} P. Miska, and M. Vergnat

Laboratoire de Physique des Matériaux, UMR CNRS 7556, Nancy University, BP 239, 54506 Vandœuvre-lès-Nancy Cedex, France

(Received 16 February 2007; accepted 20 July 2007; published online 12 September 2007)

Er-doped amorphous silicon suboxide thin films were prepared by the coevaporation method. The Er concentration was varied from 0.4 to 6 at. % and the samples were annealed at different temperatures up to 900 °C. The samples exhibit a broad photoluminescence band in the visible range. Both energy and intensity of this band were dependent on the annealing temperature. For as-deposited films and samples annealed below 500 °C, this band was assigned to defects in the oxide films. For higher annealing temperatures, this photoluminescence band shifted to higher wavelengths and was correlated to the appearance of amorphous silicon clusters. Two narrow bands in the near-infrared range at 0.98 and 1.54 μm were also observed for the annealed samples. The intensity of these Er-related luminescence was maximal for an annealing temperature equal to around 700 °C. The effective absorption cross section of Er was dependent on the annealing temperature and was equal to $6.6 \times 10^{-16} \text{ cm}^2$ for the sample annealed at 700 °C. The strong Er-related photoluminescence is discussed in terms of a coupling phenomenon between Er^{3+} ions and spatially confined amorphous silicon clusters which act as sensitizers. The existence of a low annealing temperature to obtain the best Er-related photoluminescence is also discussed. © 2007 American Institute of Physics. [DOI: 10.1063/1.2777203]

I. INTRODUCTION

Er-doped silicon-based materials have attracted much attention in the scientific community because of their potential use for optoelectronics.¹ Indeed, Er^{3+} ions can emit sharp luminescence at 1.54 μm , due to the $^4I_{13/2} \rightarrow ^4I_{15/2}$ intra- $4f$ transition, which corresponds to the minimum attenuation in the silica-based optical fibers commonly used in optical communications. Studies of Er-doped crystalline silicon (c-Si:Er) have shown that Er^{3+} ions can be efficiently excited through electron-hole pairs recombination or by impact of energetic carriers.^{2,3} The Er excitation is then characterized by an effective cross section of $3 \times 10^{-15} \text{ cm}^2$ which is five orders of magnitude higher than direct-resonant optical absorption.² However, such systems present a strong temperature quenching which is due to Auger dissociation of electron-hole pairs and energy back transfer to silicon. This thermal quenching is strongly reduced when oxygen is coimplanted and the Er luminescence yield at room temperature is improved.^{4,5} For instance, a weaker thermal quenching was observed in oxygen-doped polycrystalline or amorphous silicon which contains around 30% of oxygen.⁶

In the presence of silicon nanocrystals (Si-nc), the Er-related photoluminescence (PL) is strongly improved. This effect is attributed to a strong coupling between Er^{3+} ions and Si-nc.⁷⁻⁹ The Er^{3+} ions can then be indirectly excited by Si-nc that have an absorption cross section several orders of magnitude higher than that of direct Er excitation. Moreover, the Er nonradiative back-transfer deexcitation process is strongly reduced in presence of Si-nc, due to the widening of the band gap which produces a reduction in the free carrier

concentration. Few models describing an energy transfer from the exciton in the Si-nc to the Er^{3+} ions were proposed.^{10,11} In these models, photogenerated excitons in Si-nc can either transfer their energy to Er^{3+} ions or give rise to a luminescence in the visible range. Several Er-doped Si-based materials were prepared by evaporation,¹² chemical vapor deposition,¹³ sputtering,¹⁴ or implantation.¹⁵ To obtain a strong Er-related PL, a thermal annealing treatment at a temperature above 1000 °C is generally needed in order to create Si-nc.

However, recent results have shown that the existence of Si-nc is not necessary to obtain high Er-related PL efficiency. Indeed, it has been proposed that amorphous silicon clusters in SiO_x films can also act as efficient sensitizers for Er^{3+} ions.^{16,17} Additionally, Er luminescence was observed in Er-doped hydrogenated amorphous silicon.^{18,19} In Er-doped amorphous silicon (a-Si:Er), the PL efficiency is low at room temperature because of the existence of silicon dangling bonds,²⁰ that can be reduced by introducing hydrogen in the structure. Moreover, as in crystalline silicon, it has been reported that oxygen improves the Er luminescence.^{21,22} In these amorphous systems, the excitation of Er^{3+} ions is not clearly understood.

This work reports on the influence of the annealing temperature on the PL properties of Er-doped SiO (SiO:Er) films prepared by evaporation, up to 900 °C. Depending on the annealing temperature, different PL contributions are observed. For the as-deposited samples a broad PL band at around 550 nm is attributed to defects of the silicon oxide matrix and a very weak Er-related band at 1.54 μm is observed. With annealing treatments, the intensity of the defect band in the visible range decreases and a band with a weaker

^{a)}Electronic mail: rinnert@lpm.u-nancy.fr

intensity at higher wavelength appears, while the Er-related peak intensity increases with a maximum for an annealing temperature equal to 700 °C. A description of the Er-related light emission yield as a function of the annealing treatments is proposed and it is suggested that the formation of a-Si clusters plays an important role in the Er^{3+} ions emission.

II. EXPERIMENTAL DETAILS

A. Samples preparation

SiO_x films with x close to 1 were prepared by evaporation of SiO powder. The deposition rate was controlled by a quartz microbalance system and was equal to 1 Å/s. Er evaporation was performed from an effusion cell, allowing us to obtain low deposition rates. The temperature cell was around 1100 °C and the cell was calibrated by a quartz microbalance, allowing us to control the rare-earth content. The samples were prepared with an Er concentration in the range of 0.4–6 at. %. The Er concentration is defined by the ratio $[\text{Er}]/[\text{SiO}]$. The silicon substrates were maintained at 100 °C. For all samples, the total film thickness is equal to 200 nm. The samples were then annealed in a quartz tube with a pressure of about 10^{-9} Torr.

B. Photoluminescence characterization

Both cw and time-resolved (TR) PL experiments were performed at room temperature. For the cw experiments in the visible range, the excitation was obtained with a 200 W mercury arc lamp source, using the UV lines at 313 and 334 nm. The PL signal was analyzed by a monochromator equipped with a 150 grooves/mm grating and by a charge-coupled device camera detector cooled at 140 K. For the cw experiments in the near-infrared domain, the sample was excited by a 30 mW He–Cd laser using the 325 nm line. The PL signal was analyzed by a monochromator equipped with a 600 grooves/mm grating and by a photomultiplier tube cooled at 190 K. The power dependence of the PL was studied by using neutral density filters allowing us to change the pumping power on three orders of magnitude. For the TR-PL experiments, the sample was pumped by the 355 nm line of a frequency-tripled yttrium aluminium garnet (YAG):Nd laser. The laser pulse frequency, energy, and duration were typically equal to 10 Hz, 50 μJ , and 20 ns, respectively. The detection system is the same as that used for the cw-PL experiments in the near-infrared domain. The rise time of the detector is equal to around 10 ns. The response of the detection systems was precisely calibrated with a tungsten wire calibration source.

III. RESULTS

A. Steady state photoluminescence

Figure 1 shows the room-temperature cw-PL spectra in the range of 500–900 nm for the as-deposited SiO layer and for the layers annealed at different temperatures from 400 to 900 °C. The as-deposited sample presents a broad PL band at 550 nm. The sample annealed at 400 °C shows a PL band at the same wavelength, but with an eight times higher intensity. For higher annealing temperature, the PL band in-

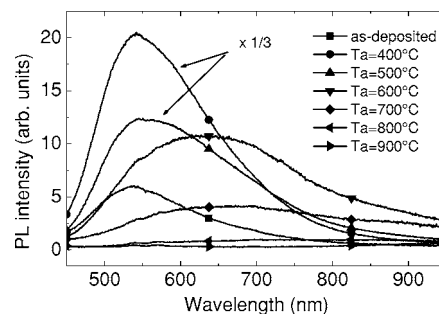


FIG. 1. Room temperature PL spectra in the range of 500–900 nm for Er-doped SiO layers annealed at different temperatures T_a . The Er concentration is equal to 0.8 at. %.

tensity decreases and the wavelength redshifts. This PL evolution is very similar to that obtained in undoped SiO layers.²³ This evolution can be interpreted by the existence of two PL bands. The first one at around 550 nm is generally attributed to the presence of defects in the SiO_x matrix, such as nonbridging oxygen hole centers.^{24,25} Its intensity increases up to 500 °C and the energy of the maximum is almost temperature independent. For annealing temperatures higher than 500 °C, this first band disappears with the suppression of the defects and a new band appears, which can be related to the phase separation process that gives rise to pure Si domains in a SiO_x matrix with x near 2, as shown in Ref. 26, following the relation $2\text{SiO} \rightarrow \text{Si} + \text{SiO}_2$. The PL band at around 700 nm is then correlated to the appearance of pure silicon embedded in a SiO_x matrix. The origin of this band is not clear, and several different origins could be proposed. It must be noted that no crystalline phase was observed in these samples, except for annealing temperature greater or equal to 950 °C.²⁷ As the size of the a-Si domains cannot be determined, no size effect can be demonstrated in these samples and it is not possible to say whether a quantum confinement effect occurs in these films. Moreover, the decay time of this band was measured and was below the detection limit of our setup, i.e., below 20 ns. This low value is not compatible with the characteristic decay time of silicon nanocrystals, which is equal to around 10 μs . The quantum confinement effect in silicon nanocrystals can be rejected as an explanation of this band. The low value of the decay time suggests that defects are implicated in the recombination process. A competition between two different processes, a nonradiative one related to defects and a radiative one related to transitions between the band tails states of spatially confined amorphous silicon clusters, cannot be rejected.

The room-temperature PL spectra in the range of 950–1650 nm are reported in Fig. 2 for the as-deposited SiO layer and for the annealed layers at different temperatures from 400 to 900 °C. No PL is observed in this spectral range for the as-deposited sample. Two Er-related bands are well visible for the annealed samples. The bands at 980 nm and 1.54 μm are characteristic of the radiative emission from the $^4I_{11/2} \rightarrow ^4I_{15/2}$ and $^4I_{13/2} \rightarrow ^4I_{15/2}$ transitions of Er^{3+} ions, respectively. The intensity of the band at 980 nm is around two orders of magnitude lower than that of the 1.54 μm band, as generally observed in similar systems. The intensity of the band at 1.54 μm is an increasing function of the annealing

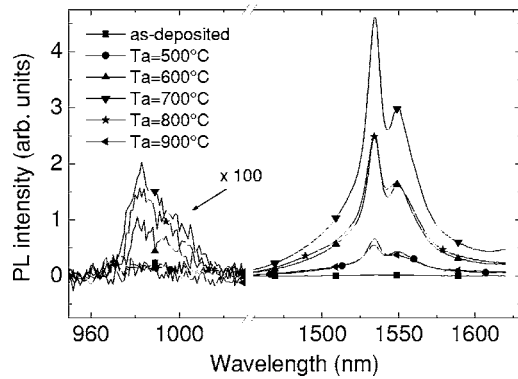


FIG. 2. Room temperature PL spectra in the range of 950–1600 nm for Er-doped SiO layers annealed at different temperatures T_a . The Er concentration is equal to 0.8 at. %.

temperature until 700 °C where the intensity is maximal. Beyond this temperature, the PL intensity decreases with the annealing temperature. The intensity of the band located at 980 nm exactly follows the same annealing temperature dependence, which clearly demonstrates a strong correlation between these two bands.

B. Decay time measurements

Time-resolved-luminescence experiments were performed at room temperature at the wavelength corresponding to the Er-related PL peak maximum, i.e., at 1.535 μm . The time dependence of the sample annealed at 700 °C is reported in Fig. 3. As for all the samples, this time dependence can be well fitted by a single exponential decrease. For the sample annealed at 700 °C, the decay time is equal to 1.5 ms, which is very close to the decay time values generally obtained in Er-doped Si-nc.^{7,28,29} The decay time was measured for the different annealing temperatures and this dependence is represented in the inset of Fig. 3. For the sample annealed at 400 °C, the decay time is equal to 0.67 ms. This decay time is an increasing function of the annealing temperature until 600 °C where it is equal to 1.5 ms. The decay time decreases for the higher annealing temperatures and reaches the value 1 ms for the sample annealed at 900 °C. Few data are given in literature concerning the evolution of the decay time with the annealing tempera-

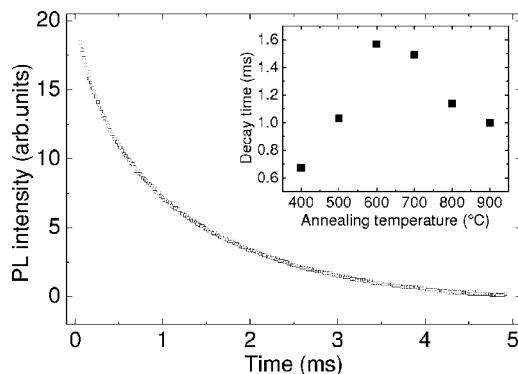


FIG. 3. Time dependence of the PL at 1.54 μm for a sample annealed at 700 °C and with an Er concentration equal to 0.8 at. %. The inset shows the evolution of the decay time with the annealing temperature.

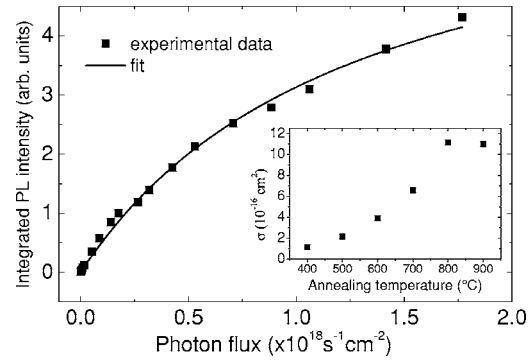


FIG. 4. Integrated PL intensity at 1.54 μm as a function of the pumping photon flux for a sample annealed at 700 °C and for an Er concentration equal to 0.8 at. %. The solid curve is a fit according to Eq. (1). The inset shows the annealing temperature dependence of the Er effective absorption cross section.

ture. In the work of Franzo *et al.*,¹⁶ the Er decay time in Er-doped Si-rich SiO₂ films was measured for samples pre-annealed from 500 to 1250 °C to generate the appearance of pure silicon domains and annealed at 900 °C after Er implantation. In this case, the decay time is nearly independent of the preannealing temperature and is equal to around 2 ms. In this present study, a clear evolution of the decay time is observed and suggests that nonradiative processes play an important role on the PL intensity.

C. Pump power dependence

The Er-related PL was measured as a function of the pump power. The evolution of the integrated PL band at 1.54 μm with the photon flux is represented in Fig. 4 for the sample annealed at 700 °C. For the low power values, the pump power dependence of the PL is linear and a saturation effect appears for the high power values. The model of energy transfer proposed by Franzo *et al.*¹⁶ that successfully describes the coupling between Si-nc and Er³⁺ ions both embedded in a SiO₂ matrix shows that the pump power dependence of the 1.54 μm PL follows a hyperbolic law according to the following expression:

$$I_{\text{PL}}/I_{\text{max}} = \sigma_{\text{eff}} \phi \tau_d^{\text{Er}} / (1 + \sigma_{\text{eff}} \phi \tau_d^{\text{Er}}), \quad (1)$$

where σ_{eff} is an effective Er absorption cross section, τ_d^{Er} is the decay time of the 1.54 μm PL, and ϕ is the pumping laser photon flux. The effective cross section is defined by the following expression:

$$\sigma_{\text{eff}} = \Lambda N \tau \sigma / \tau_{\text{tr}}^{\text{Er}}, \quad (2)$$

where N is the number of Si-nc, σ is the exciton generation cross section, τ is the recombination time of the exciton, $\tau_{\text{tr}}^{\text{Er}}$ is the transfer time from the exciton to the Er³⁺ ion, and Λ is an interaction volume which characterizes the interaction between the exciton and the Er³⁺ ion. In the present work, the same expression is applied where N is the number of confined a-Si domains. Our experimental data are perfectly fitted by the expression (1), allowing us to obtain the effective cross section of Er. Taking into account an Er decay time equal to 1.5 ms for the sample annealed at 700 °C, the value of σ_{eff} is equal to $6.6 \times 10^{-16} \text{ cm}^2$. This value is very close to

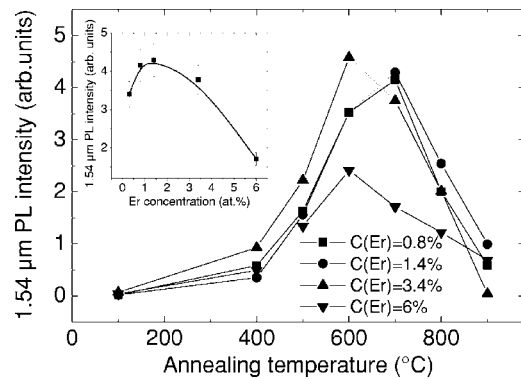


FIG. 5. Evolution of the 1.54 μm PL intensity as a function of the annealing temperature for the different Er concentrations $C(\text{Er})$. The inset shows the evolution of the 1.54 μm PL intensity as a function of the Er concentration for samples annealed at 700 $^{\circ}\text{C}$. The solid curve is a guide for the eyes.

that obtained for Er-doped Si-nc^{10,30–32} and is around four orders of magnitude higher than the cross section corresponding to the direct absorption of Er embedded in an insulating matrix.³³ The pump-power dependence of the Er-related PL was also measured for all the samples. It must be noticed that, for all the annealing temperatures, from 400 to 900 $^{\circ}\text{C}$, the expression (1) gives an excellent agreement with the experimental data. The evolution of the effective cross section of Er is represented as a function of the annealing temperature in the inset of Fig. 4. This value is an increasing function of the annealing temperature. The effective cross section of Er for the sample annealed at 900 $^{\circ}\text{C}$ is one order of magnitude higher than that of the sample annealed at 400 $^{\circ}\text{C}$.

D. Influence of the Er concentration

The Er-related PL was measured at room temperature as a function of the annealing temperature for different Er concentrations $C(\text{Er})$ from 0.4% to 6%. For all the concentrations, the evolution is similar with the existence of a PL maximum, as represented in Fig. 5. The maximum seems to depend slightly on the Er concentration. Indeed, for the high concentration values, this maximum happens at 600 $^{\circ}\text{C}$ while, for the low concentration values, this temperature is equal to 700 $^{\circ}\text{C}$.

It is also interesting to compare the Er-related PL intensity as a function of the Er concentration for the same annealing temperature. This dependence for the samples annealed at 700 $^{\circ}\text{C}$ is represented in the inset of Fig. 5. The highest PL intensity is obtained for an Er concentration equal to around 1%. For higher Er concentration, the PL intensity decreases. The PL intensity of the sample with an Er concentration equal to 6% is around three times lower than that of the sample with an Er concentration equal to 0.8%. This Er concentration dependence can be explained by a concentration quenching effect involved by nonradiative interactions between Er^{3+} ions, as already obtained in Er-doped SiO_2 samples containing Si-nc³⁴ and by the formation of optically inactive Er clusters.

The Er concentration PL dependence in the visible range was also studied and represented in Fig. 6. The PL intensity in the visible range is a decreasing function of the Er con-

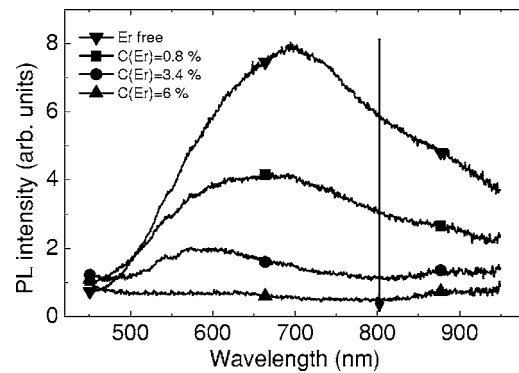


FIG. 6. Influence of the Er concentration on the PL band in the visible range for samples annealed at 700 $^{\circ}\text{C}$.

centration. By increasing this value by a factor of around 4 (from 0.8% to 3.4%), the integrated visible PL band decreases by a factor of 3. For a concentration equal to 6%, this PL band disappears. Moreover, the decrease of the PL seems more pronounced around 800 nm where a hollow appears, as shown by the arrow. A similar decrease of the PL band located at around 700 nm was obtained in Er-doped amorphous SiO_2 with the increase of Er concentration, which was interpreted by a coupling effect between a-Si clusters and the Er^{3+} ions.³⁵

IV. DISCUSSION

The evolution of the films structure with annealing treatments is important to understand the Er-related PL. Our previous results^{23,26} on undoped annealed SiO_2 layers have clearly shown that the as-deposited samples are homogeneous SiO_2 films which do not contain any detectable pure silicon phase. They also showed that pure amorphous silicon domains appear due to the phase separation of SiO_2 into pure Si and pure SiO_2 . In these previous works, the presence of a silicon phase was mainly demonstrated by infrared absorption spectrometry and by Raman experiments. Indeed, it was demonstrated that the wave number of the Si–O–Si asymmetric stretching vibration is an increasing function of the annealing treatments, showing an evolution of the silicon oxide matrix from SiO_1 to SiO_2 . As the chemical composition remained constant, this evolution is characteristic of the appearance of pure silicon in the layers. A direct signature of silicon was obtained by Raman spectroscopy which showed the characteristic transverse acoustical and transverse optical phonon modes of amorphous silicon. Due to their amorphous structure, silicon domains cannot be seen by conventional transmission electron microscopy. Moreover, other groups have recently demonstrated by energy filtered transmission electron microscopy experiments the existence of pure a-Si nanoparticles embedded in a silicon oxide matrix in annealed Si-rich SiO_2 layers.^{16,35} Let us firstly discuss the existence of a possible coupling effect between a-Si domains and Er^{3+} ions. The results show that no Er-related PL is obtained in the as-deposited samples in which no pure silicon domain is present. After an annealing process, both the a-Si domains and the Er-related PL appear, suggesting that a-Si domains could play a crucial role on the Er luminescence. Er^{3+} ions

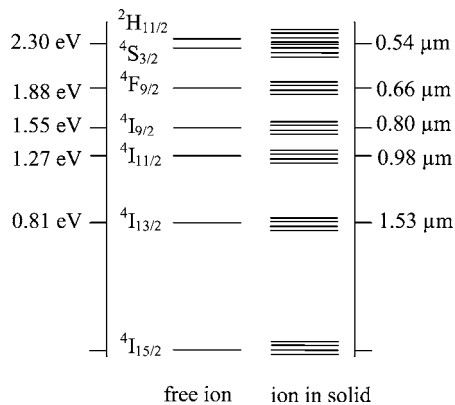


FIG. 7. Schematic energy level diagram of Er^{3+} for a free ion and for an ion in a solid. Both energies and corresponding wavelengths are given near the levels.

present different sublevels that could be responsible of the energy transfer from a-Si. The schematic energy-level diagram of Er^{3+} ions is represented in Fig. 7. Different resonant energy transfers could appear. The SiO defect band at 550 nm is resonant with the $^4S_{3/2}$ Er^{3+} electronic level. However, the coupling with this level is presumably very low because no Er-related PL is observed neither in the as-deposited sample nor in the sample annealed at 400 °C, where the PL band at 550 nm is very high.

For higher annealing temperature, the PL band in the visible range is very large and covers the $^4F_{9/2}$ and $^4I_{9/2}$ Er^{3+} electronic levels that are split due to the Stark effect. The energy of these levels corresponds to the wavelengths 660 and 800 nm. The decrease of this band when the Er concentration increases suggests that the Er ions are coupled with the luminescent centers which give rise to this broad visible band. The possible correlation between this band and a-Si clusters, as discussed beyond, could be the signature of an energy transfer from a-Si to Er^{3+} by these two energy levels, in particular, with the $^4I_{9/2}$ level, as shown by the preferential PL intensity decrease at around 800 nm. Moreover, this level was mentioned to be implicated in the energy transfer from the exciton in Si-nc to the Er^{3+} ions in Er-doped layers containing Si-nc.⁸

In the case of Er-doped Si-rich SiO_2 , an anneal at high temperature, greater than 1000 °C, is generally necessary to obtain a high Er-related PL. This high annealing temperature is needed to generate the Si-nc. In the case of Er-doped SiO layer, the best PL intensity at 1.54 μm is obtained for an anneal around 700 °C. The explanation why the maximum appears at this low temperature is not trivial because several parameters must be taken into account. First, it is generally recognized that the Er^{3+} ions must be optically activated by the presence of Er–O complexes that appear after annealing treatments. The increase of the Er-related PL can partially be explained by this complex formation.³⁶ Moreover, we have shown that the effective Er cross section is an increasing function of the annealing temperature. This increase is probably due to the SiO phase separation that produces an increasing number of pure a-Si domains. Indeed, as shown in the model described above, the effective Er cross section is proportional to the number of silicon clusters. For an Er-

doped sample with $C(\text{Er})$ equal to 0.8%, the increase of the 1.54 μm PL intensity from an anneal at 400 °C to an anneal at 700 °C is equal to 6.8 while the effective cross section has been multiplied by a factor of 6. The correlation between the effective cross section and the PL intensity at 1.54 μm is very good up to the annealing temperature of 700 °C, suggesting that the increase of the number of silicon domains is the main parameter that controls the Er-related PL intensity in this annealing-temperature range. Moreover, the measured decay time is an increasing function of the annealing temperature up to 700 °C which can be interpreted as a decrease of nonradiative recombination pathways. For higher annealing temperatures, the PL intensity decrease could be explained by several factors. A first explanation could be the phase separation process, which induces a coalescence phenomenon and then would lead to a decrease of the silicon clusters number. However, the coalescence phenomenon probably appears for annealing temperatures greater than 950 °C, as shown in Ref. 27. Moreover, the effective cross section, which is proportional to the number of domains, does not decrease for the high annealing temperatures. The decay time of the Er-related PL at 1.54 μm is a decreasing function of the annealing temperature for temperatures greater than 700 °C, which suggests that a nonradiative de-excitation process appears. This process is not clearly identified but could be due to the Er–Er interaction involved by a possible diffusion of Er in the layer, as already shown in Er-doped silica films.³⁷ This explanation could also allow us to understand why the optimal annealing temperature is lower for the high Er concentration values. Indeed, for high Er concentration, the diffusion and segregation of Er should appear for lower temperature and then lead to the decrease of the PL intensity at lower annealing temperatures.

V. CONCLUSION

Er-doped amorphous SiO_2 thin films were prepared by the coevaporation method. The influence of the annealing temperature and of the Er concentration on the PL properties was studied. Two sharp PL bands at 0.98 and 1.54 μm were assigned to the Er^{3+} ions. The high Er-related PL was interpreted by an indirect excitation process of Er from the a-Si clusters which could act as sensitizers. It is also shown that the optimal annealing temperature is equal to around 700 °C, which is far below the annealing temperature required for Er-doped samples containing Si-nc. The increase of the Er-related PL with annealing temperature up to 700 °C is assigned to an increase of the a-Si clusters number and by a decrease of nonradiative centers. Beyond 700 °C, the PL intensity decrease is attributed to the appearance of nonradiative processes such as interaction between Er atoms. The PL decay time at 1.54 μm and the effective Er absorption cross section are typically equal to 1.5 ms and 10^{-16} cm^2 , respectively. These values are very close to those obtained in Er-doped samples containing Si-nc.

¹A. Polman, J. Appl. Phys. **82**, 1 (1997).

²F. Priolo, G. Franzo, S. Coffa, and A. Carnera, Phys. Rev. B **57**, 4443 (1998).

³G. Franzo, F. Priolo, S. Coffa, A. Polman, and A. Carnera, Appl. Phys.

- Lett. **64**, 2235 (1994).
- ⁴F. Priolo, G. Franzo, S. Coffa, A. Polman, S. Libertino, R. Barklie, and D. Carey, J. Appl. Phys. **78**, 3874 (1995).
 - ⁵S. Coffa, G. Franzo, F. Priolo, A. Polman, and R. Serna, Phys. Rev. B **49**, 16313 (1994).
 - ⁶G. N. van den Hoven, J. H. Shin, A. Polman, S. Lombardo, and S. U. Campisano, J. Appl. Phys. **78**, 2642 (1995).
 - ⁷P. G. Kik, M. L. Brongersma, and A. Polman, Appl. Phys. Lett. **76**, 2325 (2000).
 - ⁸G. Franzo, D. Pacifici, V. Vinciguerra, F. Priolo, and F. Iacona, Appl. Phys. Lett. **76**, 2167 (2000).
 - ⁹M. Fujii, M. Yoshida, Y. Kansawa, S. Hayashi, and K. Yamamoto, Appl. Phys. Lett. **71**, 1198 (1997).
 - ¹⁰G. Franzo, V. Vinciguerra, and F. Priolo, Appl. Phys. A: Mater. Sci. Process. **69**, 3 (1999).
 - ¹¹A. J. Kenyon, C. E. Chryssou, C. W. Pitt, T. Shimizu-Iwayama, D. E. Hole, N. Sharma, and C. J. Humphreys, J. Appl. Phys. **91**, 367 (2002).
 - ¹²G. Wora Adeola, O. Jambois, P. Miska, H. Rinnert, and M. Vergnat, Appl. Phys. Lett. **89**, 101920 (2006).
 - ¹³J. H. Shin, M. Kim, S. Seo, and C. Lee, Appl. Phys. Lett. **72**, 1092 (1998).
 - ¹⁴M. Fujii, M. Yoshida, S. Yahashi, and K. Yamamoto, J. Appl. Phys. **84**, 4525 (1998).
 - ¹⁵C. E. Chryssou, A. J. Kenyon, T. S. Iwayama, C. W. Pitt, and D. E. Hole, Appl. Phys. Lett. **75**, 2011 (1999).
 - ¹⁶G. Franzo, S. Boninelli, D. Pacifici, F. Priolo, F. Iacona, and C. Bongiorno, Appl. Phys. Lett. **82**, 3871 (2003).
 - ¹⁷A. Meldrum, A. Hryciw, A. N. MacDonald, C. Blois, T. Clement, R. De Corby, J. Wang, and Q. Li, J. Lumin. **121**, 199 (2006).
 - ¹⁸T. Oesterreich, G. Swiatkowski, and I. Broser, Appl. Phys. Lett. **56**, 446 (1990).
 - ¹⁹M. S. Bresler *et al.*, Appl. Phys. Lett. **67**, 3599 (1995).
 - ²⁰I. N. Yassievich, M. Bresler, O. B. Gusev, J. Non-Cryst. Solids **226**, 192 (1998).
 - ²¹A. R. Zanatta, L. A. O. Nunes, and L. R. Tessler, Appl. Phys. Lett. **70**, 511 (1996).
 - ²²V. F. Masterov, F. S. Nasredinov, P. P. Seregin, V. Kh. Kudoyarova, A. N. Kuznetsov, and E. I. Terukov, Appl. Phys. Lett. **72**, 728 (1998).
 - ²³H. Rinnert, M. Vergnat, G. Marchal, and A. Burneau, Appl. Phys. Lett. **72**, 3157 (1998).
 - ²⁴A. J. Kenyon, P. F. Trwoga, C. W. Pitt, and G. Rehm, J. Appl. Phys. **79**, 9291 (1996).
 - ²⁵K. S. Min, K. V. Shcheglov, C. M. Yang, H. A. Atwater, M. L. Brongersma, and A. Polman, Appl. Phys. Lett. **69**, 2033 (1996).
 - ²⁶H. Rinnert, M. Vergnat, and A. Burneau, J. Appl. Phys. **89**, 237 (2001).
 - ²⁷O. Jambois, H. Rinnert, X. Devaux, and M. Vergnat, J. Appl. Phys. **100**, 123504 (2006).
 - ²⁸F. Gourbilleau, R. Madelon, C. Dufour, and R. Rizk, Opt. Mater. (Amsterdam, Neth.) **27**, 868 (2005).
 - ²⁹D. Pacifici, G. Franzo, F. Priolo, F. Iacona, and L. Dal Negro, Phys. Rev. B **67**, 245301 (2003).
 - ³⁰A. J. Kenyon, C. E. Chryssou, C. W. Pitt, T. Shimizu-Iwayama, D. E. Hole, N. Sharma, and C. J. Humphreys, J. Appl. Phys. **91**, 367 (2002).
 - ³¹C. C. Kao *et al.*, J. Appl. Phys. **98**, 013544 (2005).
 - ³²F. Gourbilleau, M. Levalois, C. Dufour, J. Vicen, and R. Rizk, J. Appl. Phys. **95**, 3717 (2004).
 - ³³F. Priolo, G. Franzo, D. Pacifici, V. Vinciguerra, F. Iacona, and A. Irrera, J. Appl. Phys. **89**, 264 (2001).
 - ³⁴P. G. Kik and A. Polman, J. Appl. Phys. **88**, 1992 (2000).
 - ³⁵A. Hryciw, C. Blois, A. Meldrum, T. Clement, R. De Corby, and Q. Li, Opt. Mater. (Amsterdam, Neth.) **28**, 873 (2006).
 - ³⁶F. Priolo, S. Coffa, G. Franzo, C. Spinella, A. Carnera, and V. Bellani, J. Appl. Phys. **74**, 4936 (1993).
 - ³⁷A. Polman, D. C. Jacobson, D. J. Eaglesham, R. C. Kistler, and J. M. Poate, J. Appl. Phys. **70**, 3778 (1991).